Journal of Hazardous Materials 175 (2010) 872–882

Contents lists available at ScienceDirect

Journal of Hazardous Materials

journal homepage: www.elsevier.com/locate/jhazmat

Model for a solid–liquid stirred tank two-phase partitioning bioscrubber for the treatment of BTEX

Jennifer V. Littlejohns, Kim B. McAuley, Andrew J. Daugulis*

Department of Chemical Engineering, Queen's University, Kingston, Ontario, K7L 3N6, Canada

ARTICLE INFO

Article history:
Received 15 July 2009
Received in revised form 8 October 2009
Accepted 22 October 2009
Available online 31 October 2009

Keywords:
BTEX
Solid–liquid two-phase partitioning bioreactor
Modeling
Bacterial Consortium
Biodegradation

ABSTRACT

A dynamic mathematical model has been developed to predict the performance of a stirred tank, solid–liquid two-phase partitioning bioreactor (SL-TPPB) for the treatment of benzene, toluene, ethylbenzene and o-xylene (BTEX) contaminated gases. The SL-TPPB system consists of an aqueous phase containing a bacterial consortium and a solid phase of silicone rubber beads (10%; v/v) with a high affinity for BTEX compounds. The silicone rubber beads serve to sequester and release BTEX according to thermodynamic equilibrium, which increases mass transfer from the gas phase and reduces aqueous phase concentrations of these toxic compounds during fluctuating inlet loadings. The model was developed from mass balances on BTEX components in the gas, aqueous and polymer phases, and biomass in the aqueous phase. Dynamic experimental data from this system were used to fit model parameters and to assess the accuracy of the model. A detailed estimability analysis of model parameters and initial conditions was completed to identify uncertain parameters that are most influential for the model predictions and to determine the parameters and initial conditions that should be targeted for estimation using the dynamic data. It was found that the developed model, with estimated parameters and initial conditions, has the ability to predict experimental off-gas BTEX concentrations with reasonable accuracy, which are the outputs of greatest importance.

1. Introduction

Mathematical models for biodegradation systems used in the treatment of waste gas streams serve two purposes: (1) to explain the phenomena that are occurring within the bioreactor to achieve decontamination of the waste gas stream and (2) to predict the performance of the system under various operating conditions. Recently, models have been developed and validated, with the objective of predicting performance under various operating conditions, for several novel biotreatment systems of waste gases including foamed emulsion bioreactors for the treatment of toluene [1], dual liquid-phase biofilters for hydrophobic pollutants [2], hybrid bioreactors composed of a bubble column bioreactor and biofilter compartments for the treatment of benzene [3], and membrane bioreactors for the treatment of toluene [4].

A novel biotreatment system that has been shown to be very promising for the treatment of gases contaminated by benzene, toluene, ethylbenzene and o-xylene (BTEX) is the stirred tank solid–liquid two-phase partitioning bioscrubber (SL-TPPB), which has been experimentally investigated by Littlejohns and Daugulis [5]. This system consists of an aqueous phase containing a bacterial consortium with the ability to degrade BTEX and a second nonbioavailable, immiscible and biocompatible phase of silicone rubber beads to uptake and release BTEX during dynamic operation. This uptake and release of BTEX by the polymer beads reduces toxic substrate levels in the aqueous phase during periods of high loading and increases mass transfer of BTEX out of the gas phase. Although models for liquid–liquid TPPBs for the treatment of waste gases, which have an organic solvent sequestering phase, have been developed and validated [6–9], no models exist for suspended growth SL-TPPBs, despite several benefits of using polymers as a sequestering phase over organic solvents [10].

This study discusses the development and application of such a model to predict outlet gas concentrations in a 3 L stirred tank solid–liquid TPPB for the treatment of a continuous gas stream containing BTEX. The model, which describes the experimental system studied by Littlejohns and Daugulis [5], enables improved understanding of the phenomena occurring within the system and predicts performance under various inlet loading fluctuations. Initial values for model parameters are obtained from independent experiments, empirical correlations and literature. Estimability analysis [11–13] was then performed to determine which of these

* Corresponding author at: Department of Chemical Engineering, Queen's University, 19 Division Street, Dupuis Hall, Kingston, Ontario, K7L 3N6, Canada.
Tel.: +1 613 533 2784; fax: +1 613 533 6637.
E-mail address: andrew.daugulis@chee.queensu.ca (A.J. Daugulis).

0304-3894/$ – see front matter © 2009 Elsevier B.V. All rights reserved.
doi:10.1016/j.jhazmat.2009.10.091

Nomenclature

C	substrate concentration ($mg\,L^{-1}$)
C^*	liquid equilibrium concentration ($mg\,L^{-1}$)
D	diffusion coefficient ($m^2\,s^{-1}$)
E_P	physical enhancement constant
F_g	volumetric flow rate ($L\,s^{-1}$)
H	Henry's constant ($mg\,L^{-1}\,mg^{-1}\,L$)
$I_{i2,i}$	interaction parameter for effect of substrate 2 on initial substrate
K	partition coefficient between liquid and polymer ($mg\,L^{-1}\,mg^{-1}\,L$)
K_S	half saturation constant ($mg\,L^{-1}$)
$_k$	mass transfer coefficient ($m\,s^{-1}$)
k_La	volumetric mass transfer coefficient between gas and liquid (s^{-1})
k_O	overall mass transfer coefficient between liquid and polymer ($m\,s^{-1}$)
k_d	endogenous respiration coefficient (s^{-1})
k_m	specific rate of substrate consumption for maintenance (s^{-1})
LR	loading rate ($mg\,s^{-1}$)
P_g	power input (W)
r	rate of substrate depletion ($mg\,L^{-1}\,h^{-1}$)
R	radius (m)
S_{Yr}	uncertainty in the measured responses
S_θ	uncertainty in the parameters
SR	stripping rate ($mg\,s^{-1}$)
T_i^X	growth substrate transformation capacity = mg_N/mg_G ($mg\,mg^{-1}$)
V	volume (L)
X	biomass concentration ($mg\,L^{-1}$)
Y	model output ($mg\,L^{-1}$)
$Y_{x/i}$	yield coefficient ($mg\,L^{-1}\,mg^{-1}\,L$)

Greek symbols

ε	gas hold-up
υ_s	superficial gas velocity ($m\,s^{-1}$)
ρ	density ($kg\,L^{-1}$)
μ_{max}	maximum specific growth rate (s^{-1})
ψ	proportionality factor

Subscripts

aq	sample containing aqueous phase
B	benzene
E	ethylbenzene
g	in gas phase
gl	between gas and liquid phases
HS	in the headspace of the sample
i	species B, T, E or X
in	inlet gas stream
INH	inhibitory concentration
l	in liquid phase
lp	between liquid and polymer phases
O_2	oxygen
$poly$	sample containing polymer + aqueous phase
p	in polymer phase
T	toluene
X	o-xylene

parameter values should be updated using information from the dynamic experimental data of Littlejohns and Daugulis [5], and which parameters should remain at their initial values. Estimability analysis is a formal procedure that has been used to aid parameter estimation in a variety of chemical [11–17] and biochemical [18–20] models. It selects parameters for estimation based on information about uncertainties in each of the initial parameter values, sensitivity of model predictions to the various parameters, and the quantity and quality of the dynamic experimental data. Note that uncertain initial conditions can be included as model parameters in the estimability analysis, and are selected for estimation if there is sufficient information content in the data. Using the estimability analysis, influential parameters and initial conditions were selected and were estimated to achieve improved predictions of dynamic SL-TPPB behaviour.

Table 1
List of equations.

Gas-phase balances

$$\frac{dC_{i,g}}{dt} = F_g\frac{C_{i,in}}{V_g} - E_P k_L a_i (C^*_{i,gl} - C_{i,l})\frac{V_l}{V_g} - F_g\frac{C_{i,g}}{V_g} \quad (1)$$

Liquid-phase balances

$$\frac{dC_{i,l}}{dt} = E_P k_L a_i (C^*_{i,gl} - C_{i,l}) - \frac{3k_{O,i}}{R_p}(C_{i,l} - C^*_{i,lp}) - r_i \quad (2)$$

$$\frac{dX}{dt} = r_B Y_{X/B} + r_T Y_{X/T} + r_E Y_{X/E} - k_d X \quad (3)$$

Polymer-phase balances

$$\frac{dC_{i,p}}{dt} = \frac{3k_{O,i}}{R_p}(C_{i,l} - C^*_{i,lp})\frac{V_l}{V_p} \quad (4)$$

Headspace predictions for liquid samples

$$C_{i,aq,HS} = \frac{C_{i,l} \times V_{l,aq}}{V_{g,aq} + (V_{l,aq}/H_i)} \quad (5)$$

Headspace predictions for liquid and polymer samples

$$C_{i,poly,HS} = C_{i,l} \times V_{l,poly} + \frac{C_{i,p} \times V_{p,poly}}{(V_{l,poly}/H_i) + (K_i V_{l,poly}/H_i) + V_{g,poly}} \quad (6)$$

2. Model development

In the solid–liquid stirred tank TPPB used by Littlejohns and Daugulis [5], BTEX is delivered into a well-mixed bioreactor via a continuous gas stream. The gas bubbles are dispersed throughout the bioreactor due to the agitation, and BTEX is transferred from the gas phase to the aqueous phase containing the bacterial consortium. If a build-up of BTEX occurs in the aqueous phase, for example, during feed fluctuations, BTEX partitions from the aqueous phase to the polymer beads due to thermodynamic driving forces. Alternatively, as the cells metabolize BTEX in the aqueous phase, BTEX transfers out of the polymer phase to the aqueous phase for subsequent degradation.

Table 2
Thermodynamic and kinetic expressions.

Aqueous phase in equilibrium

$$C^*_{i,gl} = C_{i,g}/H_{lg} \quad (9)$$

$$C^*_{i,lp} = C_{i,p}/K_{lp} \quad (10)$$

Microbial kinetics

$$r_B = \frac{(\mu_{max,B}C_B/((K_{s,B} + C_B) + I_{T,B}C_T + I_{X,B}C_X))(1 - (C_{B,l}/C_{B,INH}))X}{Y_{X/B}} \quad (11)$$

$$r_T = \frac{(\mu_{max,T}C_T/((K_{s,T} + C_T) + I_{B,T}C_T))(1 - (C_{T,l}/C_{T,INH}))X}{Y_{X/T}} \quad (12)$$

$$r_E = \frac{(\mu_{max,E}C_E/(K_{s,E} + C_E))(1 - (C_{E,l}/C_{E,INH}))X}{Y_{X/E}} \quad (13)$$

$$r_X = \left(\begin{array}{l}\left(T_B^X\left(\frac{dC_B}{dt}\left(\frac{1}{X}\right)\right)\right)\left(\frac{C_X}{K_{s,X} + C_X}\right)X \\ + \left(T_T^X\left(\frac{dC_T}{dt}\left(\frac{1}{X}\right)\right)\right)\left(\frac{C_X}{K_{s,X} + C_X}\right)X\end{array}\right)\left(1 - \frac{C_{X,l}}{C_{X,INH}}\right) \quad (14)$$

Table 3
Initial parameter values.

Parameter	Value	Unit	S_θ	Method of Determination
E_P	2	–	0.2	Littlejohns and Daugulis [26]
$k_L a_B$	0.0189	s^{-1}	0.00264	Shown in current study
$k_L a_T$	0.0166	s^{-1}	0.00232	Shown in current study
$k_L a_E$	0.0155	s^{-1}	0.00216	Shown in current study
$k_L a_X$	0.0155	s^{-1}	0.00216	Shown in current study
K_B	62	mg L^{-1} solid L mg^{-1} aqueous	2.88	Littlejohns and Daugulis [5]
K_T	200	mg L^{-1} solid L mg^{-1} aqueous	19.5	Littlejohns and Daugulis [5]
K_E	414	mg L^{-1} solid L mg^{-1} aqueous	153.08	Littlejohns and Daugulis [5]
K_X	593	mg L^{-1} gas L mg^{-1} aqueous	86.4	Littlejohns and Daugulis [5]
H_B	0.26	mg L^{-1} gas L mg^{-1} aqueous	0.04	Littlejohns and Daugulis [5]
H_T	0.35	mg L^{-1} gas L mg^{-1} aqueous	0.02	Littlejohns and Daugulis [5]
H_E	0.43	mg L^{-1} gas L mg^{-1} aqueous	0.02	Littlejohns and Daugulis [5]
H_X	0.25	mg L^{-1} gas L mg^{-1} aqueous	0.03	Littlejohns and Daugulis [5]
$K_{o,B}$	1.05×10^{-8}	m s^{-1}	1.84×10^{-6}	Shown in current study
$K_{o,T}$	9.3×10^{-9}	m s^{-1}	1.63×10^{-6}	Shown in current study
$K_{o,E}$	8.5×10^{-9}	m s^{-1}	1.48×10^{-6}	Shown in current study
$K_{o,X}$	8.5×10^{-9}	m s^{-1}	1.48×10^{-6}	Shown in current study
ε	0.09	–	0.02	Calderbank [27]
$\mu_{max,B}$	0.00012	s^{-1}	0.0018	Littlejohns and Daugulis [25]
$\mu_{max,T}$	0.00017	s^{-1}	0.0023	Littlejohns and Daugulis [25]
$\mu_{max,E}$	0.000036	s^{-1}	0.006	Littlejohns and Daugulis [25]
$K_{s,B}$	27.57	mg L^{-1}	11.01	Littlejohns and Daugulis [25]
$K_{s,T}$	34.12	mg L^{-1}	12.12	Littlejohns and Daugulis [25]
$K_{s,E}$	0.36	mg L^{-1}	1.76	Littlejohns and Daugulis [25]
$K_{s,X}$	0.1	mg L^{-1}	10	Littlejohns and Daugulis [25]
$I_{T,B}$	2	–	0.5	Littlejohns and Daugulis [25]
$I_{X,B}$	−0.7	–	0.5	Littlejohns and Daugulis [25]
$I_{B,T}$	−0.4	–	0.5	Littlejohns and Daugulis [25]
$I_{E,B}$	4	–	0.5	Littlejohns and Daugulis [25]
$C_{B,INH}$	20	mg L^{-1}	15	Abuhamed et al. [28]
$C_{T,INH}$	20	mg L^{-1}	15	Abuhamed et al. [28]
$C_{E,INH}$	35	mg L^{-1}	15	Estimated from Abuhamed et al. [28]
$C_{X,INH}$	35	mg L^{-1}	15	Estimated from Abuhamed et al. [28]
$Y_{X/B}$	1.35	mg mg^{-1}	0.27	Littlejohns and Daugulis [25]
$Y_{X/T}$	1.25	mg mg^{-1}	0.25	Littlejohns and Daugulis [25]
$Y_{X/E}$	0.85	mg mg^{-1}	0.17	Littlejohns and Daugulis [25]
$T_B{}^X$	0.5	–	0.1	Littlejohns and Daugulis [25]
$T_T{}^X$	0.5	–	0.1	Littlejohns and Daugulis [25]
k_d	2.5×10^{-6}	s^{-1}	0.000001	Shown in current study

The model for the SL-TPPB was developed using the following key assumptions:

1. The contents of each phase in the reactor (gas, liquid, polymer) are of uniform BTEX concentration and composition.
2. BTEX is transferred from the gas phase to the aqueous phase, and from the aqueous phase to the polymer phase [21]. Direct transfer between the gas phase and the polymer is neglected.
3. The biomass is distributed throughout the liquid and consumes BTEX only from the aqueous phase.
4. All polymer beads are spherical and are the same size.
5. The diffusion coefficients of BTEX in the polymer are constant.
6. Constant partition coefficients describe equilibrium between the liquid and polymer phases. Henry's law describes equilibrium between the gas and liquid phases.
7. Concentration gradients develop within the polymer particles during dynamic operation, in response to dynamic changes in BTEX concentrations in the aqueous phase. Instead of predicting these gradients and the associated diffusion rates explicitly using partial differential equations, mass transfer from the particles can be adequately described using inside-the-particle mass transfer coefficients that have been developed and used for other types of reactors that contain polymer particles [22,23].
8. Substrate toxicity can be described using the model by Luong [24].
9. Substrate interactions can be described using the model by Littlejohns and Daugulis [25].
10. Oxygen levels are sufficiently high so that biological reactions are not oxygen limited.
11. A lumped overall mass transfer coefficient can describe BTEX mass transfer from the liquid to polymer phases.
12. The resistance to BTEX mass transfer in the gas phase and microbial cell walls is negligible.

Table 4
Experimental conditions.

Operational conditions	Total BTEX loading rate (mg(L^{-1} h^{-1}))	Inlet concentration (mg L^{-1}) of total BTEX[a]	Flow rate (L h^{-1})
Nominal	60	5.36	33.6
Two times nominal	120	10.72	33.6
Four times nominal	240	21.44	33.6
Six times nominal	360	32.16	33.6
Ten times nominal	600	53.6	33.6

[a] All BTEX components are present in approximately equal concentrations.

Table 5
Ranking and parameter estimates.

Estimability rank	Parameter/initial condition	Upper/lower bounds	Estimated value	Units
1	$K_{s,X}$	1/0.001	0.005375	mg L^{-1}
2	$\mu_{max,E}$	0.00036/3.6 × 10^{-6}	3.641 × 10^{-6}	s^{-1}
3	$\mu_{max,B}$	0.0012/1.2 × 10^{-5}	6.103 × 10^{-5}	s^{-1}
4	$C_{E,in,2}$	0.5/0.01	0.02	mg L^{-1}
5	$C_{E,in,4}$	0.5/0.01	0.02	mg L^{-1}
6	$C_{E,in,10}$	0.5/0.01	0.16	mg L^{-1}
7	$\mu_{max,T}$	0.0017/1.7 × 10^{-5}	3.209 × 10^{-5}	s^{-1}
8	$C_{E,in,6}$	0.5/0.01	0.05	mg L^{-1}
9	$k_{o,X}$	6.5 × 10^{-10}/5.5 × 10^{-6}	1.4 × 10^{-7}	m s^{-1}
10	$k_L a_B$	0.00189/0.189	0.0789	s^{-1}
11	$k_L a_T$	0.00166/0.166	0.0766	s^{-1}
12	$k_L a_X$	0.00155/0.155	0.0355	s^{-1}
13	H_T	0.45/0.20	0.22	–
14	$C_{Bio,in,4}$	7000/9000	8500.53	mg L^{-1}
15	$C_{Bio,in,6}$	6000/8000	7451	mg L^{-1}
16	$C_{Bio,in,10}$	7000/9000	7200	mg L^{-1}
17	$C_{Bio,in,2}$	5000/7000	6568.53	mg L^{-1}
18	$I_{T,B}$	–	–	–
19	$C_{E,INH}$	–	–	mg L^{-1}
20	$I_{E,B}$	–	–	–

13. Mass transfer of BTEX to/from the headspace to/from the liquid is negligible.
14. Physical enhancement of mass transfer due to the presence of solids, E_P, is identical for each BTEX component, and is the same as that for oxygen estimated by Littlejohns and Daugulis [26].
15. Temperature and pH are constant.

Table 1 contains the set of equations used to model the system. Mass balances on BTEX components in each phase were used to develop ordinary differential equations to describe BTEX concentrations in the gaseous, liquid and polymer phase, which are listed in Table 1 as Eqs. (1), (2) and (4), respectively. The outlet gas BTEX concentrations determine the performance of the SL-TPPB (as the objective of the system is the treatment of contaminated gases) and were the primary interest in the current study. The concentration of biomass in the aqueous phase is represented in Table 1 by Eq. (3). A term for o-xylene contributing to biomass growth is not present in Eq. (3) due to previous research showing that o-xylene is cometabolized by the bacterial consortium [25]. During the dynamic experiments, aqueous samples and aqueous + polymer samples were removed from the reactor and were allowed to reach phase equilibrium, to provide information about BTEX concentrations in the aqueous and polymer phases [5]. Eqs. (5) and (6) are included in the model so that these headspace measurements can be used to obtain information about the model parameters.

Table 2 contains thermodynamic and kinetic expressions that were substituted into the primary equations listed in Table 1. The thermodynamic expressions that are used to determine concentrations in the aqueous phase in equilibrium with the gas phase and the polymer phase are listed as Eqs. (9) and (10), respectively, in Table 2. Kinetic expressions that were developed previously [25] in combination with the model by Luong [24] to account for substrate toxicity are shown in Table 2 as Eqs. (11)–(14) for benzene, toluene, ethylbenzene and o-xylene, respectively.

3. Materials and methods

3.1. Parameter values

Parameter values were obtained from independent experiments, empirical correlations, and/or literature values, and are listed in Table 3. The following section outlines how the parameters listed as "Shown in current study" were obtained from experiments and correlations.

3.1.1. Experiments for parameter values

The experiments that were performed in this study allowed for the determination of diffusivity of BTEX components into the polymer ($D_{p,B}$, $D_{p,T}$, $D_{p,E}$, and $D_{p,X}$) and the specific rate of consumption for maintenance (k_m) and were used in correlations to obtain model parameter values.

3.1.1.1. Materials. Benzene and toluene were obtained from Sigma–Aldrich (Oakville, Canada) and ethylbenzene and o-xylene were obtained from Fisher Scientific (Nepean, Canada). Silicone rubber, primarily composed of polydimethylsiloxane, was obtained from GE (Huntersville, NC) in the form of 100% silicone rubber caulking which was dried to spherical beads of density 1.15 g L^{-1} and diameter 2.2 mm. BTEX compounds were used during the determination of $D_{p,B}$, $D_{p,T}$, $D_{p,E}$ and $D_{p,X}$ as described in Section 3.1.1.4.1. These diffusivities were used in the determination of overall mass transfer coefficients for BTEX between aqueous and

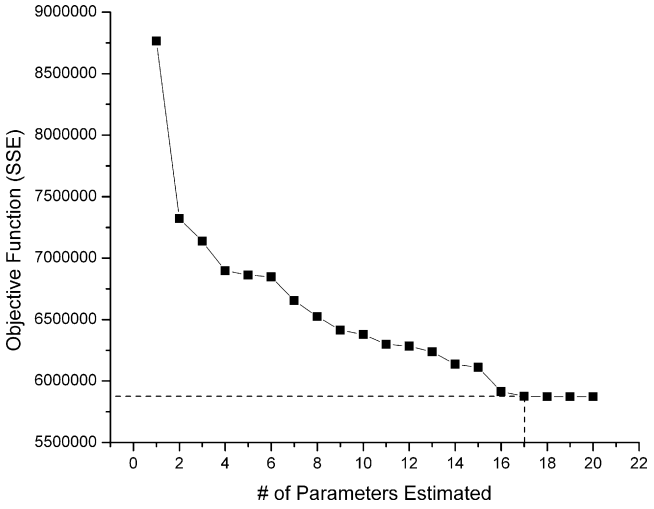

Fig. 1. Objective function for increasing number of parameters and initial conditions estimated.

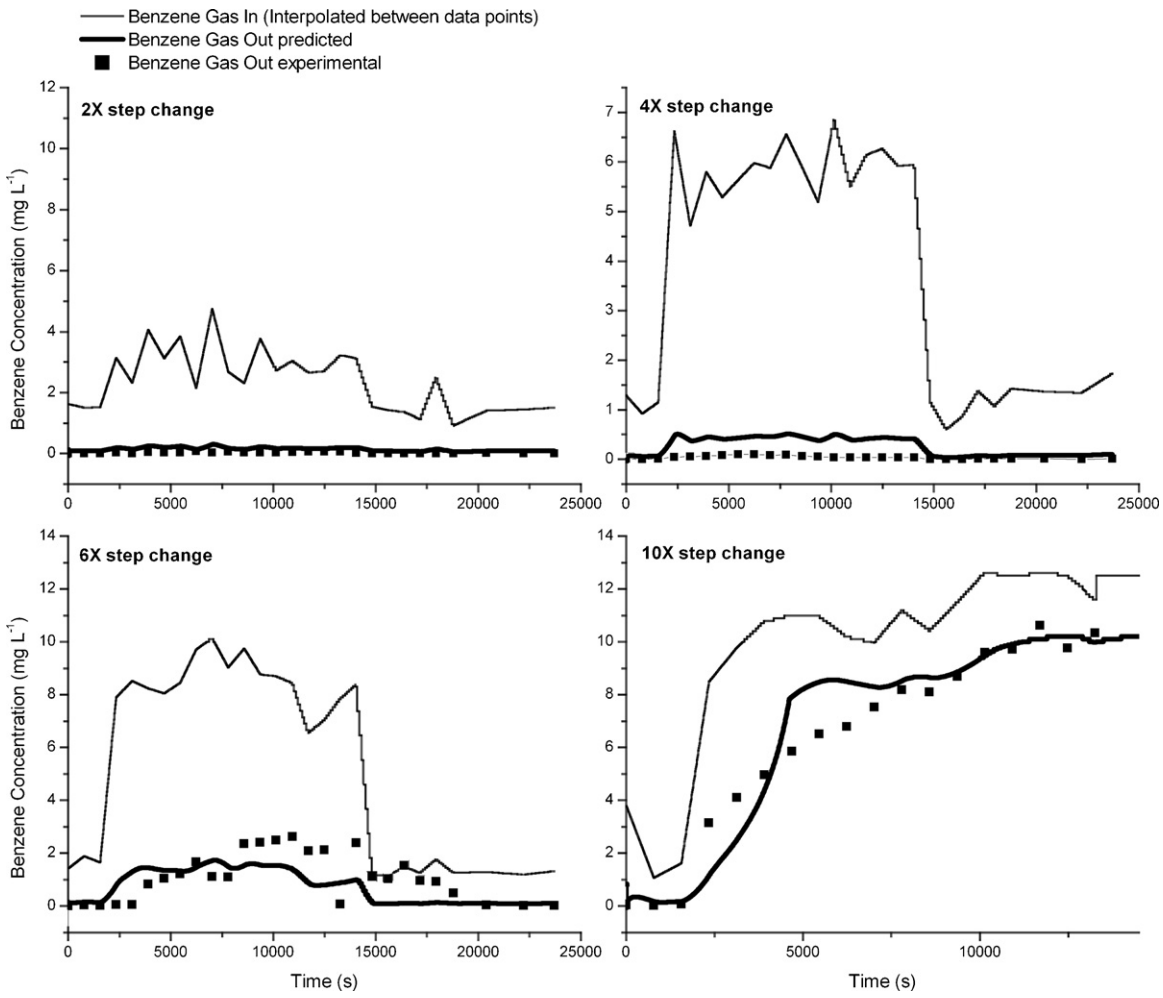

Fig. 2. Predicted and experimental benzene concentrations in gas streams over a range of step change conditions.

polymer phases ($k_{o,B}$, $k_{o,T}$, $k_{o,E}$, $k_{o,X}$) as described in Section 3.1.2.2. BTEX compounds and silicone rubber beads were used in the determination of k_m, as described in Section 3.1.1.4.2, which was used in the determination of the endogenous respiration coefficient (k_d) as described in Section 3.1.2.4.

3.1.1.2. Microorganisms. The bacterial consortium was enriched from petroleum-contaminated soil as previously described in Littlejohns and Daugulis [25]. A denaturing gradient gel electrophoresis performed by Microbial Insights (Rockford, TN) revealed the consortium used in this study consists of seven different species of *Pseudomonas*. These microorganisms were used during the determination of k_m, as described in Section 3.1.1.4.2, which was used in the determination of k_d, as described in Section 3.1.2.4.

3.1.1.3. Equipment. To determine k_m, as described in Section 3.1.1.4.2, the bioreactor used was a NewBrunswick Bioflo III with a 3 l working volume of aqueous media of identical composition to that used in Littlejohns and Daugulis [5]. Air was diffused through flasks containing BTEX components, which were combined with makeup air to create a gaseous stream containing BTEX. The bioreactor was operated at identical conditions to the TPPB being modeled in the current study, and was therefore automatically maintained at a temperature of 30 °C, a pH of 6.9 and agitated at 800 rpm.

3.1.1.4. Experimental procedure.

3.1.1.4.1. Diffusion coefficients of BTEX in silicone rubber, $D_{p,B}$, $D_{p,T}$, $D_{p,E}$, $D_{p,X}$. The diffusion coefficients for BTEX species in silicone rubber were determined experimentally by adding 3 g silicone rubber into a sealed 125 ml amber bottle filled to the top with aqueous medium. 5 μl of each BTEX component was injected into the aqueous medium, and the amber bottle was maintained at 30 °C and agitated at 180 rpm. Periodic 1 ml measurements of the aqueous phase were taken using a gas-tight syringe, through self-sealing septa at the top of the bottle, which were injected into 2 ml gas tight containers. These containers were left to equilibrate for 1 h, at which time the gas phase concentrations in the 2 ml containers were measured using GC/FID. The method for GC/FID is explained elsewhere [25]. The concentration of BTEX absorbed into the polymer at the time the sample was taken from the amber bottle was then calculated using Henry's constants. Diffusion coefficients were then determined using the method described by Amsden et al. [10], and were used in Section 3.1.2.2, in order to determine $k_{o,B}$, $k_{o,T}$, $k_{o,E}$, and $k_{o,X}$.

3.1.1.4.2. Specific rate of consumption for maintenance, k_m. To determine k_m, BTEX was delivered to the single-phase bioscrubber via a continuous gas stream containing BTEX at a loading of 60 mg L^{-1} h^{-1} with approximately equal amounts of each compound until the system reached steady-state (>200 h). Gas samples of the inlet and outlet gas streams, along with biomass samples were taken approximately every 12 h. Gas samples were analyzed

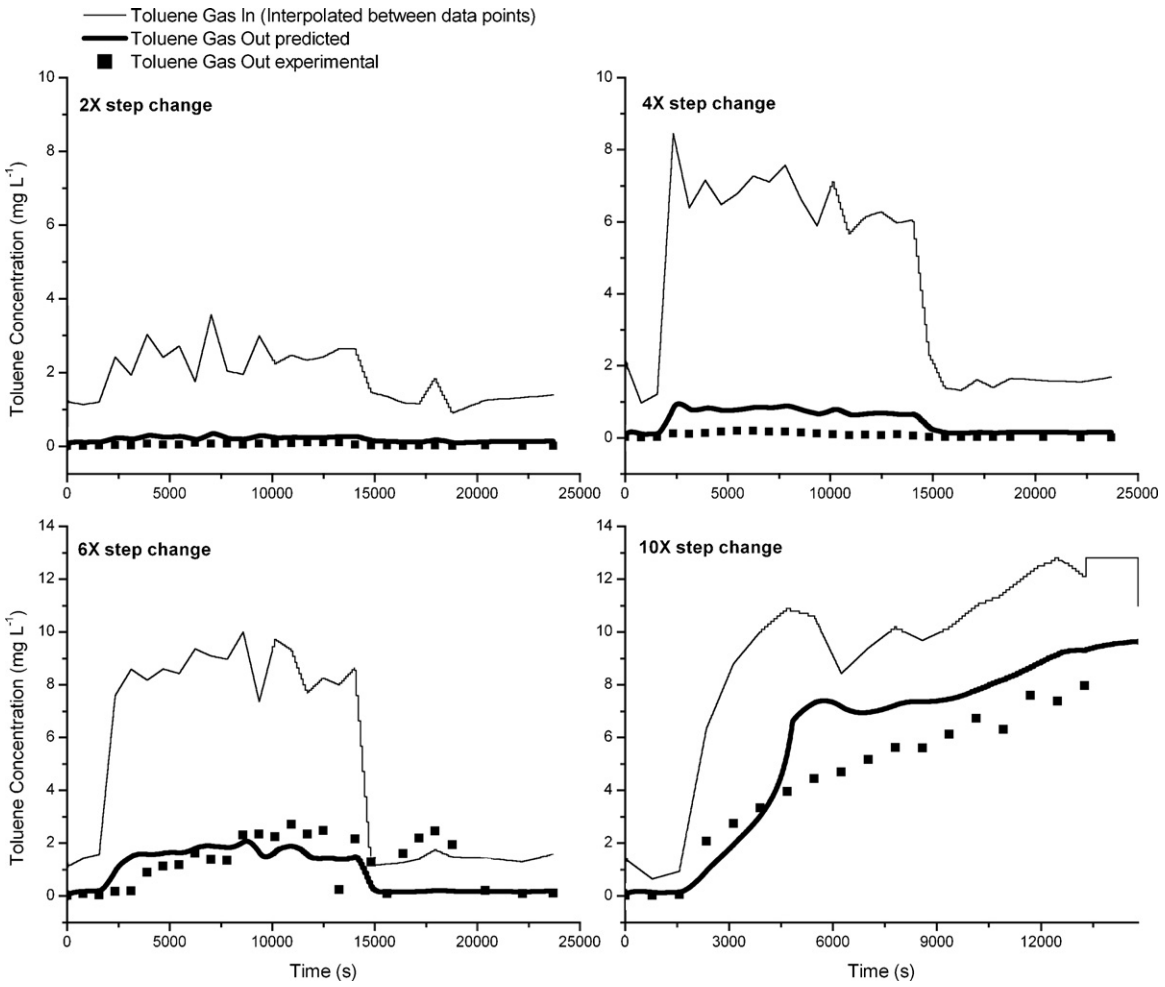

Fig. 3. Predicted and experimental toluene concentrations in gas streams over a range of step change conditions.

using GC/FID and biomass concentrations were analyzed using optical density measurements using methods described elsewhere [25]. Once the system had reached steady state, Eq. (15) was applied [29]:

$$k_m = \frac{LR - SR}{X \cdot V_l} \tag{15}$$

where LR and SR are the loading and stripping rates in mg s^{-1}, respectively, as defined in the nomenclature section. This value was used in Section 3.1.2.4, to determine k_d.

3.1.2. Correlations for parameter values

The correlations used in this study utilized experimental values determined in the current study, along with literature values, and allowed for the determination of volumetric mass transfer coefficients for BTEX (k_La_B, k_La_T, k_La_E, k_La_X), overall mass transfer coefficients for BTEX between aqueous and polymer phases ($k_{o,B}$, $k_{o,T}$, $k_{o,E}$, $k_{o,X}$), entrained gas volume (ε) and the endogenous respiration coefficient (k_d).

3.1.2.1. Volumetric mass transfer coefficients, k_La_B, k_La_T, k_La_E, k_La_X. The experimental methodology used for determining physical enhancement coefficients and volumetric oxygen mass transfer coefficients in a stirred tank reactor are described in Littlejohns and Daugulis [26]. These volumetric oxygen mass transfer coefficients were used to determine volumetric BTEX mass transfer coefficients using the correlation shown in Eq. (16) [30]:

$$k_La_i = \psi \cdot k_La_{O_2} \tag{16}$$

The parameter ψ was estimated using Eq. (17) [31]:

$$\psi = \frac{D_i}{D_{O_2}} \tag{17}$$

Diffusion coefficients used in Eq. (14) for oxygen and BTEX in water at 30 °C are 3.51×10^{-5}, 1.17×10^{-5}, 1.03×10^{-5}, 9.33×10^{-6} and 9.33×10^{-6} cm^2 s^{-1}, respectively [32].

3.1.2.2. Overall mass transfer coefficients for BTEX between aqueous and polymer phases, $k_{o,B}$, $k_{o,T}$, $k_{o,E}$, $k_{o,X}$. The overall mass transfer coefficient for BTEX between aqueous and polymer phases must consider both aqueous and polymer resistances to mass transfer. The overall mass transfer coefficient was calculated using Eq. (18) [22]:

$$\frac{1}{k_{O,i}} = \frac{1}{K_i k_{p,i}} + \frac{1}{k_{l,i}} \tag{18}$$

In order to determine mass transfer coefficients on the liquid and polymer sides, semi-empirical equations can be used which are shown as Eq. (19) [22] and Eq. (20), respectively [23]:

$$k_{l,i} = \frac{D_{i,l}}{R_p} \tag{19}$$

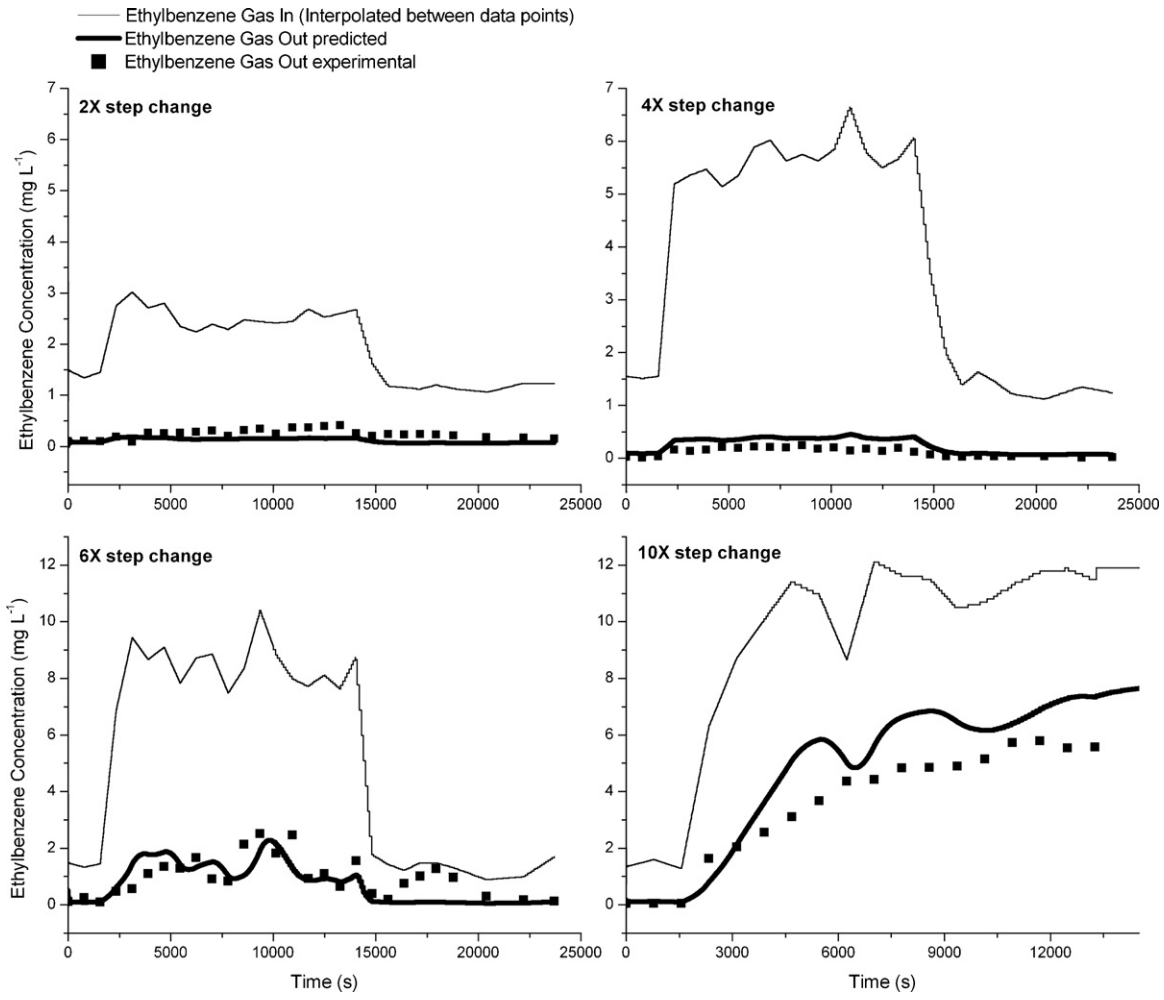

Fig. 4. Predicted and experimental ethylbenzene concentrations in gas streams over a range of step change conditions.

$$k_{p,i} = \frac{D_{i,p}\pi^2}{2R_p} \tag{20}$$

3.1.2.3. Entrained gas volume, ε. Gas holdup in the reactor was estimated using the correlation seen in Eq. (21) [27], which was used to determine the entrained gas volume in the system:

$$\varepsilon = 1.8 * Pm^{0.14} \upsilon_s^{0.5} \tag{21}$$

where $P_m = P_g/\rho V_l$ and $\varepsilon = V_g/V_g + V_l$.

3.1.2.4. Endogenous respiration coefficient, k_d. The maintenance requirements for the system were modeled using the specific endogenous respiration coefficient, as it provides more realistic predictions compared to the specific rate of substrate consumption for maintenance [33]. However, both approaches account for the same macroscopic observation and are related by Eq. (22), which was used to determine the parameter value of k_d

$$k_d = Y_{X/i} k_m \tag{22}$$

3.2. Modeling

3.2.1. Solid–liquid TPPB data

The experimental data for pseudo steady-state and dynamic operation of the solid–liquid TPPB that are modeled in the current study was obtained previously as described in Littlejohns and Daugulis [5]. The experimental data for the dynamic conditions modeled were obtained after operation of the SL-TPPB until pseudo steady-state biomass concentrations were reached (>200 h). The approximate operating conditions that were used to obtain the modeled experimental data are listed in Table 4 for step changes of 2, 4, 6 and 10 times nominal BTEX loadings. The data being modeled consist of operation at a nominal BTEX loading during pseudo-steady state for approximately 30 min, followed by a dynamic loading step change for approximately 230 min, followed by a return to nominal loading for approximately 150 min. Inlet concentrations fluctuated considerably during data collection due to minor increases or decreases in the rotameter settings.

3.2.2. Numerical methods

Matlab™ was used to generate model predictions by numerical integration of the differential Eqs. (1), (2) and (4) for each BTEX compound and Eq. (3) for biomass, using the solver ode23s. The period of operation that was modeled includes steady-state operation at nominal loading, followed by a dynamic step change, followed by a return to nominal loading at conditions described in Section 3.2.1. The model was solved for step changes of 2, 4, 6 and 10 times the nominal loading. The initial conditions for each equation that were input into the ODE solver were determined by experimental measurements at steady-state operation prior to each step change. However, as there is experimental error present in the measured initial condition values, these initial conditions were also treated as parameters during estimability analysis and parameter estimation.

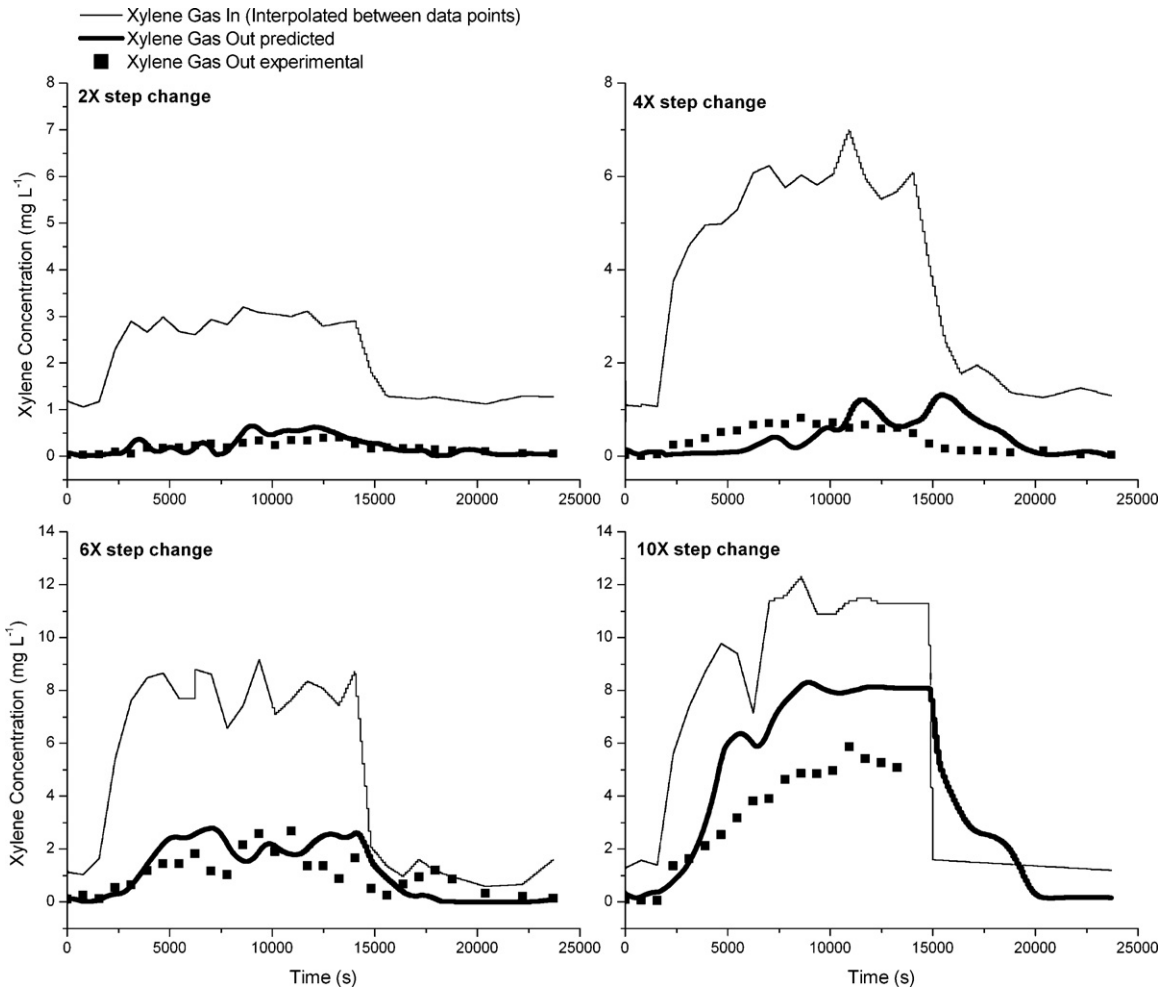

Fig. 5. Predicted and experimental xylene concentrations in gas streams over a range of step change conditions.

As stated previously, inlet concentrations fluctuated during experimental operation due to minor increases or decreases in the rotameters. Therefore, to model these fluctuations, BTEX inlet concentration used in the model were approximated using measured experimental data and by interpolating between the each sequential inlet sample concentration to model periods between samples. As little experimental data exist beyond $t = 150$ min for the step change to 10 times the nominal loading, predictions beyond this point were not determined and used for parameter estimation.

Parameter and initial condition estimates, as described in the following section, were determined by finding the parameter values that minimize the objective function which was the weighted sum of squared errors between the model predictions and the experimental measurements for BTEX concentrations in the outlet gas, headspace in the aqueous phase samples, headspace in the aqueous + polymer phase samples, and biomass concentrations using the "lsqnonlin" Matlab™ routine.

3.2.3. Estimability analysis and parameter estimation

An estimability analysis of the 43 parameters in the model and 52 initial condition inputs was completed to determine which parameters and initial conditions had the largest impact on model predictions. This analysis was followed by estimation of the most important parameters (and initial conditions) within realistic upper and lower bounds to obtain more precise values than provided by the initial parameter values and experimental measurements of initial conditions, and to improve the accuracy of the model predictions. The estimability analysis ranked the parameters and initial conditions according to their influence on model outputs, their correlation with other model parameters and uncertainty in initial values, using the method described by Thompson et al. [13]. During the estimability analysis, the sensitivity coefficients were scaled using uncertainties S_θ in the initial parameter values and S_{Yr} in the measured responses [13,15]. The scaling factors S_θ in Table 3 provided information to the estimability algorithm concerning how precisely the initial parameter values could be estimated from the independent data (e.g. from the experiments described in Section 3.1.1.4). Using this information, the estimability algorithm selected parameters with large uncertainty and large influence for re-estimation using the dynamic SL-TPPB data. Parameters that could be determined precisely from the preliminary experiments or that had little influence on the predictions of the dynamic data were not re-estimated, but were kept at their initial values shown in Table 3.

The estimability analysis resulted in a list of parameters ranked from most estimable to least estimable. Parameters and initial conditions that were ranked highest on the list are those that are most estimable from the available data, because these parameters have large initial uncertainties, large influences on model predictions and have little correlation with the effects of other parameters that rank higher on the list. These high ranking parameters and initial conditions were, therefore, the targets for estimation using experimental data from the SL-TPPB runs. The parameter values in Table 3 and measured initial conditions were used as the initial guesses

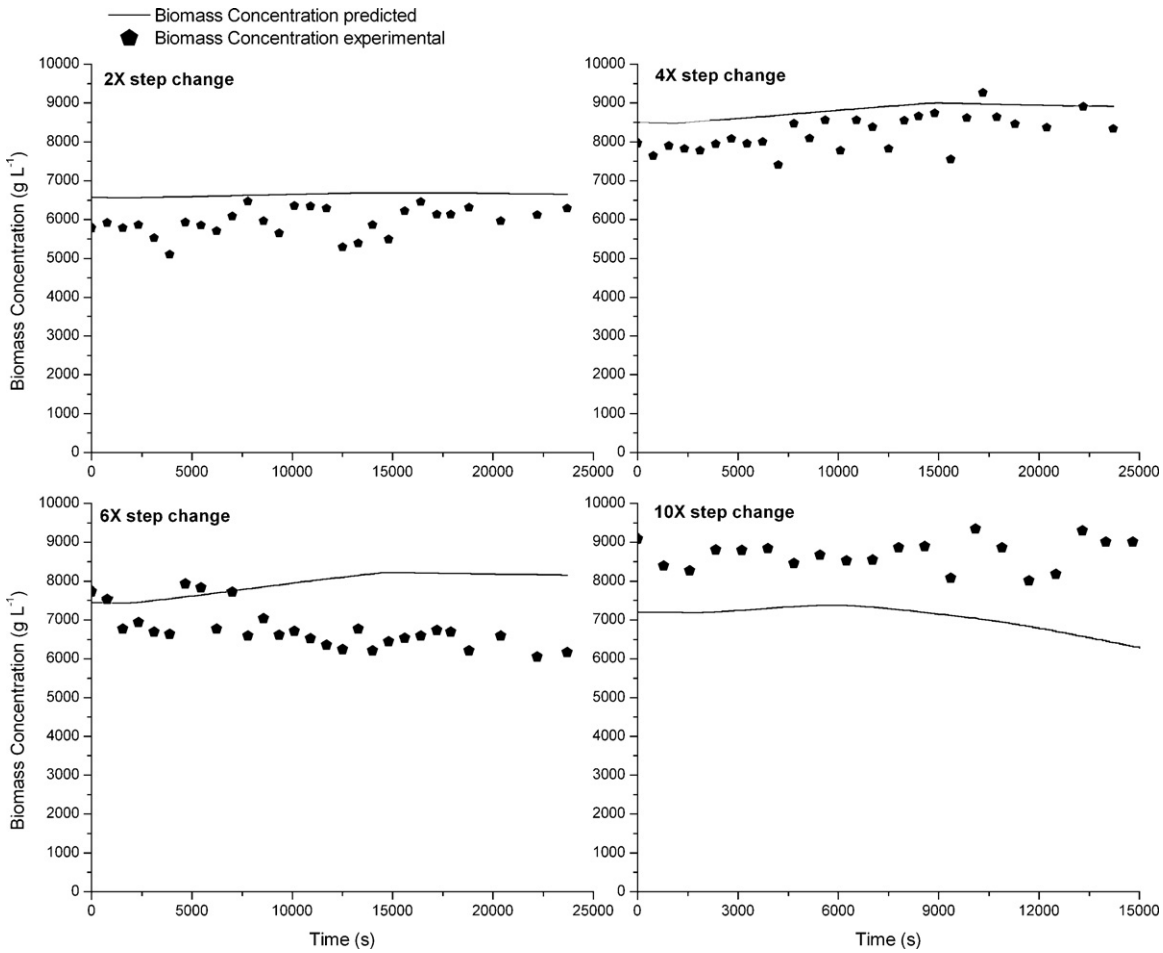

Fig. 6. Predicted and experimental biomass concentrations over a range of step change conditions.

for estimation, and the model predictions were fit to the experimental data by minimizing an objective function that consisted of the sum of squared errors weighted by uncertainties in the different types of experimental measurements. Upper and lower bounds (see Table 5) on the estimated parameters and initial conditions were enforced during the parameter estimation to ensure that all estimated values remained physically realistic. A series of parameter estimation calculations were performed, beginning with the most estimable parameter, ($K_{s,X}$, by itself) followed by the two most estimable parameters ($K_{s,X}$, and $\mu_{max,E}$) then the three and so on. Parameter estimation stopped when including additional parameters did not cause a noticeable decrease in the objective function for parameter estimation.

4. Results and discussion

4.1. Estimability analysis and parameter estimation

The parameters and initial conditions that were identified to have the largest impact on model output were identified by the estimability analysis and are ranked in Table 5. From the information provided by experimental step change SL-TPPB runs, it was determined that at least 20 parameters or initial conditions could be estimated. It can be seen that the most influential parameters are those that govern the rate of biological degradation, which might be expected, as biological uptake is the only true sink for BTEX components in the system and its rate can govern the driving force between phases. $K_{s,X}$ was found to have the largest impact on model predictions, possibly partially due to the relatively large uncertainty associated with the original value of the parameter. The initial conditions for ethylbenzene concentration in the gas phase are also shown to be influential to the model predictions. This could be due to the fact that ethylbenzene has a relatively large interaction with benzene degradation (see $I_{E,B}$ in Table 3) and all other species interact with benzene. Other model parameters and initial conditions that are highly estimable include gas–liquid mass transfer coefficients and initial biomass concentrations. Gas–liquid mass transfer is relatively rapid in comparison to other system dynamics, which accounts for these parameters being highly ranked. Biomass concentrations are slow to respond to step changes, which explains why initial conditions of biomass concentration would be influential to the model predictions.

In order to determine the optimal number of parameters and initial conditions to estimate, the estimation routine was repeated using an increasing number of parameters and initial conditions in the order of rank shown in Table 5. The weighted sum of squared errors between the experimental data and model predictions as a function of the number of parameters estimated can be seen plotted in Fig. 1. This figure shows that after estimating the top 17 parameters and initial conditions, model predictions do not improve noticeably. Therefore, 17 parameters and initial conditions were estimated, whose values can be seen in Table 5. One of the important observations is that the maximum specific growth rates that were estimated are an order of magnitude lower than the original values. This may be possibly attributed to a change in the population distribution and kinetics of the micro-

bial consortium from the time these kinetic values were initially determined [25] until the experimental step changes were performed [5], as it is known that microbial consortia populations can change during the length of time of biodegradation experiments [34]. Also, biological activity from short shake flask experiments may not reflect biological activity during lengthy bioreactor runs.

4.2. Model predictions

The model predictions for the outlet gas concentration were of primary interest in this study, as reduction of outlet BTEX concentrations is the objective of the treatment system. Figs. 2–5 show the inlet concentrations (inputs into the model) and the experimental and predicted outlet gas concentrations for benzene, toluene, ethylbenzene and o-xylene, respectively, for nominal loadings at steady state, followed by 4-h step changes of 2*X*, 4*X*, 6*X* and 10*X* the nominal loadings, with a subsequent return to nominal loadings. It can be seen that the model predictions are successful in accurately predicting the off-gas behavior during these dynamic periods for all compounds. However, for benzene and toluene during the 4*X* step change, the off-gas concentration was slightly over-predicted. In addition, for benzene, toluene and ethylbenzene during the 6*X* step change, the model predicts that the system returns to nominal off-gas concentrations upon completion of the step change slightly faster than the experimental data. Overall, the model has the ability to predict that substrate toxicity occurs during the 10*X* step change, as outlet concentrations increase significantly, however, xylene concentrations in the outlet gas were slightly over-predicted.

The predictions and experimental data for biomass concentrations over all step changes are shown in Fig. 6. It can be seen that the biomass concentrations are accurately predicted for step changes of 2*X* and 4*X*. For the 6*X* step change, biomass is slightly over-predicted, particularly near the end of the step change. Possibly this may account for the under-predicting of benzene, toluene and ethylbenzene gas concentrations after the completion of the 6*X* step change, as seen in Figs. 2–4, respectively. The biomass concentration was under-predicted during the 10*X* run, as the biomass was predicted to decline during the step change, however, as the technique used to measure biomass concentrations does not distinguish between viable and non-viable cells, the experimental biomass concentrations appeared to stay relatively constant.

The developed model has been shown to predict dynamic experimental data that range from the system completely damping out step change loading fluctuations to the system succumbing to substrate toxicity, with reasonable accuracy. It should be noted that biofilm formation would change the model structure and predictions significantly. However, it has been shown by Amsden et al. [10] that biofilm formation does not occur on polymers in a mechanically agitated TPPB, and was therefore not included in the model in the current study. Future work in this area should be focused on validating this model under varying inlet flow rates and polymer volume fractions. In addition, the use of this model to predict system performance under various polymer volume fractions or mixing conditions could allow for identification of favourable operating regions. This well-mixed model provides a framework and select parameter estimates for models of more complex SL-TPPBs that cannot be assumed to be well-mixed, such as airlift reactors.

5. Conclusions

A mechanistic model of a stirred tank SL-TPPB for the treatment of gaseous BTEX has been presented with the primary objective of predicting outlet gas concentrations. Experimental data obtained from operation of this system over dynamic step change conditions was used to estimate parameters and assess model accuracy. As estimability analysis of the model parameters and initial conditions allowed for the identification of those values that have the most significant impact on model output, which were found to be those that influenced biological activity. After the estimation of the identified model parameters and initial conditions, the model was able to predict dynamic experimental data with reasonable accuracy. The model is capable of predicting a range of responses from the SL-TPPB including completely damping out inlet fluctuations during smaller inlet loading step changes, to the system succumbing to toxic aqueous concentrations during larger inlet loading step changes.

Acknowledgement

The financial support of the Natural Sciences and Engineering Research Council of Canada is gratefully acknowledged.

References

[1] E. Kan, M.A. Deshusses, Modeling of a foamed emulsion bioreactor. I. Model development and experimental validation, Biotechnol. Bioeng. 99 (2008) 1096–1106.
[2] M.H. Fazaelipoor, Analysis of a dual liquid phase biofilter for the removal of hydrophobic organic compounds from airstreams, Chem. Eng. J. 147 (2008) 110–116.
[3] S.H. Yeom, A simplified steady-state model of a hybrid bioreactor composed of a bubble column bioreactor and biofilter compartments, Process Biochem. 42 (2007) 554–560.
[4] E. England, M.W. Fitch, M. Mormile, M. Roberts, Toluene removal in membrane bioreactors under recirculating and non-recirculating liquid conditions, Clean Technol. Environ. Policy 7 (2005) 259–269.
[5] J.V. Littlejohns, A.J. Daugulis, Response of a solid–liquid two-phase partitioning bioreactor to transient BTEX loadings, Chemosphere 73 (2008) 798–804.
[6] M.H. Fazaelipoor, A model for treating polluted air streams in a continuous two-liquid phase stirred tank bioreactor, J. Hazard. Mater. 148 (2007) 453–458.
[7] M. Koutinas, I.I.R. Baptista, A. Meniconi, L.G. Peeva, A. Mantalaris, P.M.L. Castro, A.G. Livingston, The use of an oil-absorber-bioscrubber system during biodegradation of sequentially alternating loadings of 1,2-dichloroethane and fluorobenzene in a waste gas, Chem. Eng. Sci. 62 (2007) 5989–6001.
[8] D.R. Nielsen, A.J. Daugulis, P.J. McLellan, Dynamic simulation of benzene vapor treatment by a two-phase partitioning bioscrubber. Part I. Model development, parameter estimation, and parametric sensitivity, Biochem. Eng. J. 36 (2007) 239–249.
[9] D.R. Nielsen, A.J. Daugulis, P.J. McLellan, Dynamic simulation of benzene vapor treatment by a two-phase partitioning bioscrubber. Part II. Model calibration, validation, and predictions, Biochem. Eng. J. 36 (2007) 250–261.
[10] B.G. Amsden, J. Bochanysz, A.J. Daugulis, Degradation of xenobiotics in a partitioning bioreactor in which the partitioning phase is a polymer, Biotechnol. Bioeng. 84 (2003) 399–405.
[11] K.Z. Yao, B.M. Shaw, B. Kou, K.B. McAuley, Modeling ethylene/butene copolymerization with multi-site catalysis: parameter estimability and experimental design, Polym. React. Eng. 11 (2003) 563–588.
[12] B. Kou, K.B. McAuley, C.C. Hsu, C.C. Hsu, D.W. Bacon, K.Z. Yao, Mathematical model and parameter estimation for gas-phase ethylene homopolymerization with supported metallocene catalyst, Ind. Eng. Chem. Res. 44 (2005) 2428–2442.
[13] D.E. Thompson, K.B. McAuley, P.J. McLellan, Parameter estimation in a simplified MWD model for HDPE produced by a Ziegler–Natta catalyst, Macromol. React. Eng. 3 (2009) 160–177.
[14] J.E. Puskas, S. Shaikh, K.Z. Yao, K.B. McAuley, G. Kaszas, Kinetic simulation of living carbocationic polymerizations II. Simulation of living isobutylene polymerization using a mechanistic model, Eur. Polym. J. 41 (2005) 1–14.
[15] B. Kou, K.B. McAuley, J.C.C. Hsu, D.W. Bacon, Mathematical model and parameter estimation for gas-phase ethylene-hexene copolymerization with metallocene catalyst, Macromol. Mater. Eng. 290 (2005) 537–557.
[16] B.R. Jayasankar, A. Ben-Zvi, B. Huang, Identifiability and estimability study for a dynamic solid oxide fuel cell model, Comput. Chem. Eng. 33 (2009) 484–492.
[17] V.I. Koeva, S. Daneshvar, R.J. Senden, A.H.M. Imam, L.J. Schreiner, K.B. McAuley, Mathematical modeling of PAG and NIPAM-based polymer gel dosimeters contaminated by oxygen and inhibitor. Macromol. Theory Simul., doi:10.1002/mats.200900023.
[18] K.G. Gadkar, J. Varner, F.J. Doyle III, Model identification of signal transduction networks from data using a state regulator problem, Syst. Biol. 2 (2005) 17–30.
[19] T. Quaiser, M. Monningmann, Systematic identifiability testing for unambiguous mechanistic modeling—application to JAK-STAT, MAP kinase, and NF-κB signaling pathway models, Systems Biol. 3 (2009) 50, article.

[20] J.V. Littlejohns, K.B. McAuley, A.J. Daugulis, Model for a solid–liquid airlift two-phase partitioning bioscrubber for the treatment of BTEX, J. Chem. Tech. Biotech., doi:10.1002/jctb.2280.
[21] R.L. Kars, R.J. Best, A.A.H. Drinkenburg, The sorption of propane in slurries of activated carbon in water, Chem. Eng. J. 17 (1997) 201–210.
[22] J.W. Ma, M.F. Cunningham, K.B. McAuley, B. Keoshkerian, M.K. Georges, Interfacial mass transfer in nitroxide-mediated miniemulsion polymerization, Macromol. Theory Simul. 11 (2002) 953–960.
[23] K.Z. Yao, K.B. McAuley, E.K. Marchildon, Simulation of continuous solid-phase polymerization of nylon 6,6. III. Simplified model, J. Appl. Polym. Sci. 89 (2003) 3701–3712.
[24] J.H.T. Luong, Generalization of monod kinetics for analysis of growth data with substrate inhibition, Biotechnol. Bioeng. 29 (1987) 242–248.
[25] J.V. Littlejohns, A.J. Daugulis, Kinetics and interactions of BTEX compounds during degradation by a bacterial consortium, Process Biochem. 43 (2008) 1068–1076.
[26] J.V. Littlejohns, A.J. Daugulis, Oxygen transfer in a gas–liquid system containing solids of varying oxygen affinity, Chem. Eng. J. 129 (2007) 67–74.
[27] P.H. Calderbank, Physical rate processes in industrial fermentation. Part I. The interfacial area in gas–liquid contacting with mechanical agitation, Chem. Eng. Res. Des. 36 (1958) 443–463.
[28] T. Abuhamed, E. Bayrakter, T. Mehmetoğlu, ÜT. Mehmetoğlu, Kinetics model for growth of *Pseudomonas putida* F1 during benzene, toluene and phenol biodegradation, Process Biochem. 39 (2004) 983–988.
[29] D.R. Nielsen, A.J. Daugulis, P.J. McLellan, Quantifying maintenance requirements from the steady-state operation of a two-phase partitioning bioscrubber, Biotechnol. Bioeng. 90 (2005) 248–258.
[30] Metcalf and Eddy Inc., Wastewater Engineering: Treatment, Disposal, Reuse, McGraw-Hill, New York, 1991.
[31] J. Nielsen, J. Villadsen, Bioreaction Engineering Principles, Plenum Publishing, New York, 1994.
[32] EPA (U.S. Environmental Protection Agency), Diffusion Coefficient Estimation—Extended Input Range, 2007.
[33] J.A. Roels, Energetics and Kinetics in Biotechnology, Elsevier Biomedical Press, New York, 1983.
[34] I.I.R. Baptista, N.Y. Zhou, E.A.C. Emanuelsson, L.G. Peeva, D.J. Leak, A. Mantalaris, A.G. Livingston, Evidence of species succession during chlorobenzene biodegradation, Biotechnol. Bioeng. 99 (2008) 68–74.